ENDF-177

ORNL-TM-3974
(ENDF-177)

SDT7. EXPERIMENT ON SECONDARY GAMMA-RAY PRODUCTION CROSS SECTIONS AVERAGED OVER A FAST-NEUTRON SPECTRUM FOR IRON, STAINLESS STEEL, OXYGEN, AND SODIUM

R. E. Maerker

OAK RIDGE NATIONAL LABORATORY
OPERATED BY UNION CARBIDE CORPORATION • FOR THE U.S. ATOMIC ENERGY COMMISSION

This report was prepared as an account of work sponsored by the United States Government. Neither the United States nor the United States Atomic Energy Commission, nor any of their employees, nor any of their contractors, subcontractors, or their employees, makes any warranty, express or implied, or assumes any legal liability or responsibility for the accuracy, completeness or usefulness of any information, apparatus, product or process disclosed, or represents that its use would not infringe privately owned rights.

ORNL-TM-3974
(ENDF-177)

Contract No. W-7405-eng-26

Neutron Physics Division

SDT7. Experiment on Secondary Gamma-Ray Production Cross Sections Averaged Over a Fast-Neutron Spectrum for Iron, Stainless Steel, Oxygen, and Sodium

R. E. Maerker

Reference: R. E. Maerker and F. J. Muckenthaler, "Gamma-Ray Spectra Arising from Fast-Neutron Interactions in Elements Found in Soil, Concretes, and Structural Materials," ORNL-4475 (1969).

OCTOBER 1972

OAK RIDGE NATIONAL LABORATORY
Oak Ridge, Tennessee 37830
operated by
Union Carbide Corporation
for the
U.S. ATOMIC ENERGY COMMISSION

Abstract

The experimental and calculational details for a CSEWG integral data testing shielding experiment are presented. This particular experiment measured the secondary gamma-ray production cross sections averaged over a fast-neutron spectrum for iron, a type 321 stainless steel, oxygen, and sodium. Production cross sections were binned into ∿ 0.5-MeV wide gamma-ray energy intervals.

Description

Gamma-ray production cross sections arising from fast-neutron interactions for iron, stainless steel, oxygen, and sodium were obtained in 0.5-MeV bins from gamma-ray spectra measurements described in the reference. These measurements were made at the Oak Ridge National Laboratory Tower Shielding Facility using a carefully calibrated 5 x 5 in. NaI(Tℓ) detector in good geometry. The experimental arrangement is shown in Fig. 1.

Experimental Data

The experimental data are differential in the gamma-ray energy from approximately 1 to 6.5 MeV and are expressed as values of 4π times the differential gamma-ray production cross section at 90 degrees to the incident neutron beam averaged over all neutron energies lying above 1 MeV. Gamma-ray production measurements for iron, stainless steel, oxygen, and sodium are given in Tables IA through VA. These results are estimated to have an accuracy of ±30% and include the contributions from both discrete and continuum gamma rays. The tabulated relative fast-neutron spectra for each experiment are given in Tables IB through VB.

Methods of Calculation

No transport calculations are necessary for this benchmark, hence model description, atom densities, etc. are not needed. Averaging can be done as follows:

Let $P(\Delta E_n)$ be the entries in the tabulated relative fast-neutron spectrum. Then for the continuum or unresolved contribution to the production cross section,

$$\overline{\sigma}_c(\Delta E\ ) = \sum_{\Delta E_n} P(\Delta E_n)\, \overline{\sigma}_c(\Delta E_n, \Delta E_\gamma) \quad ,$$

where

$$\sigma_c(\Delta E_n, \Delta E_\gamma) = \int_{\Delta E_n} \sigma_c(E_n, \Delta E_\gamma)\, dE_n / \Delta E_n \quad .$$

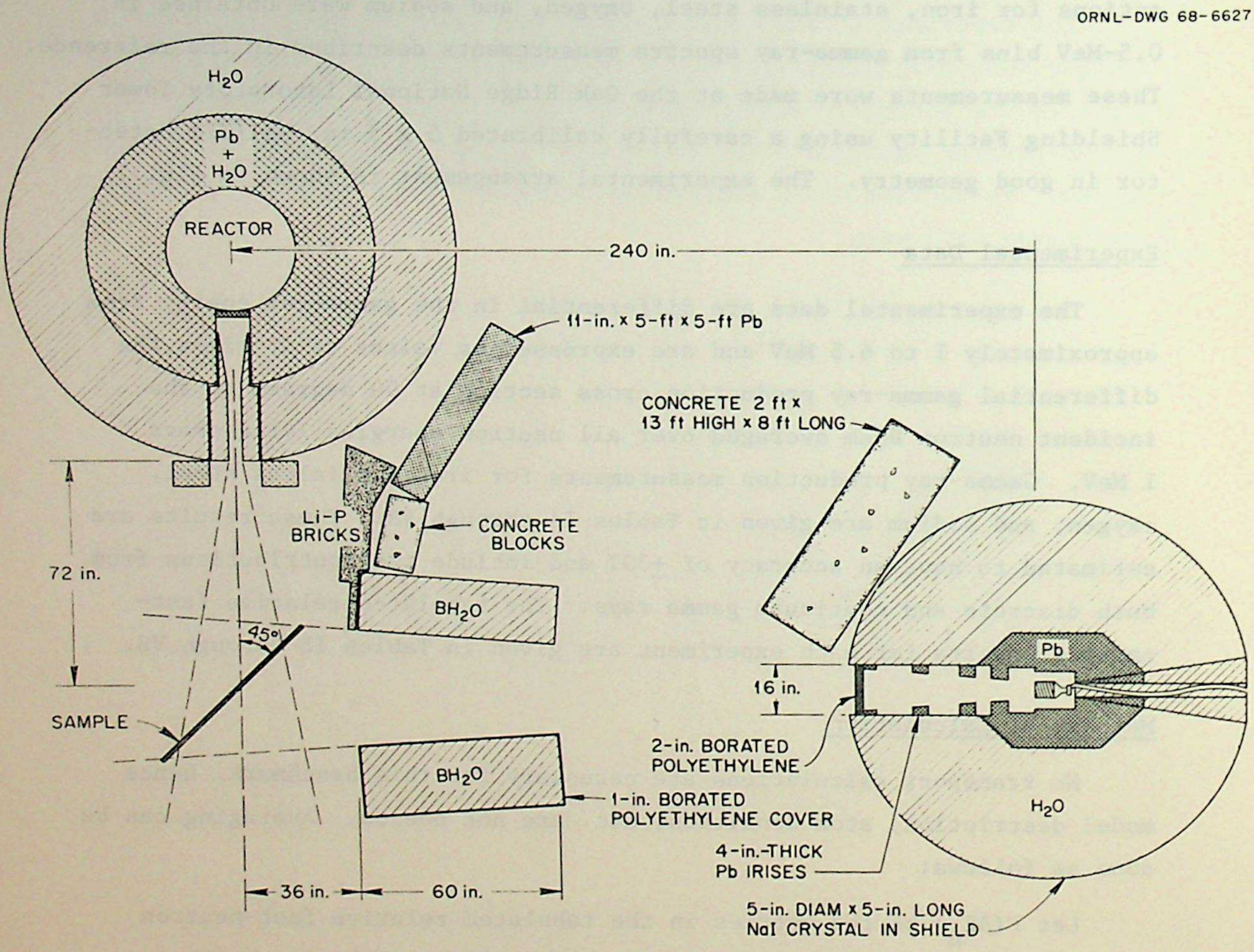

Fig. 1. Schematic Diagram of Geometry for Determining Average Secondary Gamma-Ray Production Cross Sections from Fast-Neutron Interactions. In addition, a 6-in. thickness of lithium hydride, not shown, was placed in the detector beam between the slab and the detector collimator.

The evaluation of the integral depends on the neutron energy grid of the ENDF/B data, and may have to be rather coarsely estimated.

Similarly, for the discrete contribution to the production cross section,

$$\overline{\sigma}_d(E_\gamma) = \sum_{\Delta E_n} P(\Delta E_n)\, \overline{\sigma}_d(\Delta E_n, E_\gamma) \quad ,$$

where

$$\overline{\sigma}_d(\Delta E_n, E_\gamma) = \int_{\Delta E_n} \sigma_d(E_n, E_\gamma)\, dE_n/\Delta E_n \quad ,$$

and again the accuracy of the evaluation of this integral depends on the neutron energy grid of the data.

Finally,

$$\overline{\sigma}(\Delta E_\gamma) = \overline{\sigma}_c(\Delta E_\gamma) + \sum_{\Delta E_\gamma} \sigma_d(E_\gamma) \quad ,$$

and it is this value that is to be compared with experiment.

It is recommended, however, that a "standard" ENDF/B photon production group averaging code such as LAPHANO (written by Los Alamos) or LAPHFØR (Oak Ridge's modified version of LAPHANO) be used to accomplish the above.

The input for LAPHANO or LAPHFØR, for example, is relatively straightforward. Note the following input items:

NGG = number of gamma groups = 14 (see Table IA);

NGF = number of neutron fine groups = 18 (see Table IB);

NBF = number of neutron broad groups = 1.

The gamma energy bounds are given in Table IA and the neutron energy bounds and weighting spectrum are given in Table IB. The neutron broad group is specified from 1 to 14 MeV, which covers the energy region of interest. The MT flag is set to call for all reactions given in the files. All other flags for numbers of nuclides, mixtures, zones, etc.

are set for one material, one mixture, one zone with radius = 1.0 etc. Note that the cross sections are outputted in barns.*

Method of Reporting

The calculational results should be tabulated as shown in Tables IV through IX.

*Acknowledgments should be made to R. J. LaBauve of Los Alamos Scientific Laboratory and W. E. Ford III of Oak Ridge National Laboratory for the general description of the input for the LAPHANO and LAPHFØR processing codes.

Table I

A. Experimental values of 4π times the differential gamma-ray production cross sections at 90° averaged over the tabulated fast-neutron spectrum for iron are the following, in millibarns:

Gamma-Ray Energy Interval (MeV) *	Average Cross Section (mb)
1.0 - 1.5	278
1.5 - 2.0	132
2.0 - 2.5	101
2.5 - 3.0	74
3.0 - 3.5	44
3.5 - 4.0	33
4.0 - 4.5	8.7
4.5 - 5.0	5.6
5.0 - 5.5	3.8
5.5 - 6.0	2.4
6.0 - 6.5	< 2.1
6.5 - 7.0	< 0.6
7.0 - 7.5	< 1.5
≥ 7.5	0

*Upper energy limit of each group not included in summation.

B. Tabulated relative fast-neutron spectrum:

Neutron Energy Group (MeV)	Relative Number in Group	Neutron Energy Group (MeV)	Relative Number in Group
1.0 - 1.5	0.174	5.5 - 6.0	0.026
1.5 - 2.0	0.163	6.0 - 6.5	0.021
2.0 - 2.5	0.169	6.5 - 7.0	0.015
2.5 - 3.0	0.118	7.0 - 7.5	0.011
3.0 - 3.5	0.079	7.5 - 8.0	0.008
3.5 - 4.0	0.063	8.0 - 9.0	0.009
4.0 - 4.5	0.056	9.0 - 10.0	0.005
4.5 - 5.0	0.045	10.0 - 12.0	0.003
5.0 - 5.5	0.034	12.0 - 14.0	0.001
Totals 1.0 - 14.0			1.000

Table II

A. Experimental values of 4π times the differential gamma-ray production cross sections at 90° averaged over the tabulated fast-neutron spectrum for stainless steel (67.4 weight percent iron, 18.3 weight percent chromium, 9.7 weight percent nickel, 1.5 weight percent manganese, and the remainder may be neglected) are the following, in millibarns:

Gamma-Ray Energy Interval (MeV)*	Average Cross Section (mb)
1.0 - 1.5	383
1.5 - 2.0	139
2.0 - 2.5	84
2.5 - 3.0	53
3.0 - 3.5	43
3.5 - 4.0	25
4.0 - 4.5	8.8
4.5 - 5.0	5.8
5.0 - 5.5	5.1
5.5 - 6.0	3.0
6.0 - 6.5	< 2.6
6.5 - 7.0	< 4.9
≥ 7.5	0

*Upper energy limit of each group not included in summation.

B. Tabulated relative fast-neutron spectrum:

Neutron Energy Group (MeV)	Relative Number in Group	Neutron Energy Group (MeV)	Relative Number in Group
1.0 - 1.5	0.174	5.5 - 6.0	0.026
1.5 - 2.0	0.163	6.0 - 6.5	0.021
2.0 - 2.5	0.169	6.5 - 7.0	0.015
2.5 - 3.0	0.118	7.0 - 7.5	0.011
3.0 - 3.5	0.079	7.5 - 8.0	0.008
3.5 - 4.0	0.063	8.0 - 9.0	0.009
4.0 - 4.5	0.056	9.0 - 10.0	0.005
4.5 - 5.0	0.045	10.0 - 12.0	0.003
5.0 - 5.5	0.034	12.0 - 14.0	0.001
Totals 1.0 - 14.0			1.000

Table III

A. Experimental value of 4π times the differential gamma-ray production cross section at 90° averaged over the tabulated fast-neutron spectrum for the 6.13-MeV gamma ray in oxygen is the following, in millibarns:

Gamma-Ray Energy (MeV)	Average Cross Section (mb)
6.13	90

B. Tabulated relative fast-neutron spectrum for the 6.13-MeV gamma-ray production test

Neutron Energy Group (MeV)	Relative Number in Group	Neutron Energy Group (MeV)	Relative Number in Group
6.5 - 7.0	0.290	10.5 - 11.0	0.018
7.0 - 7.5	0.204	11.0 - 11.5	0.013
7.5 - 8.0	0.150	11.5 - 12.0	0.009
8.0 - 8.5	0.107	12.0 - 12.5	0.006
8.5 - 9.0	0.075	12.5 - 13.0	0.004
9.0 - 9.5	0.054	13.0 - 13.5	0.003
9.5 - 10.0	0.038	13.5 - 14.0	0.002
10.0 - 10.5	0.027		
Totals 6.5 - 14.0			1.000

Table IV

A. Experimental value of 4π times the differential gamma-ray production cross section at 90° averaged over the tabulated fast-neutron spectrum for the 6.92 + 7.12 MeV gamma rays in oxygen is the following, in millibarns:

Gamma-Ray Energy (MeV)	Average Cross Section (mb)
6.92 + 7.12	55

B. Tabulated relative fast-neutron spectrum for the production test for 6.92 + 7.12 MeV gamma rays

Neutron Energy Group (MeV)	Relative Number in Group	Neutron Energy Group (MeV)	Relative Number in Group
7.4 - 7.5	0.063	10.5 - 11.0	0.034
7.5 - 8.0	0.278	11.0 - 11.5	0.024
8.0 - 8.5	0.198	11.5 - 12.0	0.016
8.5 - 9.0	0.139	12.0 - 12.5	0.012
9.0 - 9.5	0.099	12.5 - 13.0	0.008
9.5 - 10.0	0.069	13.0 - 13.5	0.006
10.0 - 10.5	0.050	13.5 - 14.0	0.004
Totals 7.4 - 14.0			1.000

Table V

A. Experimental values of 4π times the differential gamma-ray production cross sections at 90° averaged over the tabulated fast-neutron spectrum for sodium are the following, in millibarns:

Gamma-Ray Energy Interval (MeV)*	Average Cross Section (mb)
1.1 - 1.5	59
1.5 - 2.0	131
2.0 - 2.5	47
2.5 - 3.0	50
3.0 - 3.5	22
3.5 - 4.0	15
4.0 - 4.5	7.3
4.5 - 5.0	4.6
5.0 - 5.5	2.9
5.5 - 6.0	3.7
6.0 - 6.5	4.2
6.5 - 7.5	2.4
≥ 7.5	0

*Upper energy limit of each group not included in summation.

B. Tabulated relative fast-neutron spectrum:

Neutron Energy Group (MeV)	Relative Number in Group	Neutron Energy Group (MeV)	Relative Number in Group
1.0 - 1.5	0.174	5.5 - 6.0	0.026
1.5 - 2.0	0.163	6.0 - 6.5	0.021
2.0 - 2.5	0.169	6.5 - 7.0	0.015
2.5 - 3.0	0.118	7.0 - 7.5	0.011
3.0 - 3.5	0.079	7.5 - 8.0	0.008
3.5 - 4.0	0.063	8.0 - 9.0	0.009
4.0 - 4.5	0.056	9.0 - 10.0	0.005
4.5 - 5.0	0.045	10.0 - 12.0	0.003
5.0 - 5.5	0.034	12.0 - 14.0	0.001
Totals 1.0 - 14.0			1.000

Table VI

Report sheet for values of 4π times the differential gamma-ray production cross sections at 90° averaged over the tabulated fast-neutron spectrum for iron:

Gamma-Ray Energy Interval (MeV)*	Average Cross Section (mb)
1.0 - 1.5	______
1.5 - 2.0	______
2.0 - 2.5	______
2.5 - 3.0	______
3.0 - 3.5	______
3.5 - 4.0	______
4.0 - 4.5	______
4.5 - 5.0	______
5.0 - 5.5	______
5.5 - 6.0	______
6.0 - 6.5	______
6.5 - 7.0	______
7.0 - 7.5	______
≥	______

*Do not include upper energy limit of each group in summation.

Table VII

Report sheet for values of 4π times the differential gamma-ray production cross sections at 90° averaged over the tabulated fast-neutron spectrum for stainless steel:

Gamma-Ray Energy Interval (MeV)*	Average Cross Section (mb)
1.0 - 1.5	______
1.5 - 2.0	______
2.0 - 2.5	______
2.5 - 3.0	______
3.0 - 3.5	______
3.5 - 4.0	______
4.0 - 4.5	______
4.5 - 5.0	______
5.0 - 5.5	______
5.5 - 6.0	______
6.0 - 6.5	______
6.5 - 7.5	______
$\geq$ 7.5	______

*Do not include upper energy limit of each group in summation.

Table VIII

Report sheet for values of 4π times the differential gamma-ray production cross sections at 90° averaged over the tabulated fast-neutron spectra for oxygen:

Gamma-Ray Energy (MeV)	Average Cross Section (mb)
6.13	______
6.92 + 7.12	______

Table IX

Report sheet for values of 4π times the differential gamma-ray production cross sections at 90° averaged over the tabulated fast-neutron spectrum for sodium:

Gamma-Ray Energy Interval (MeV)*	Average Cross Section (mb)
1.1 - 1.5	______
1.5 - 2.0	______
2.0 - 2.5	______
2.5 - 3.0	______
3.0 - 3.5	______
3.5 - 4.0	______
4.0 - 4.5	______
4.5 - 5.0	______
5.0 - 5.5	______
5.5 - 6.0	______
6.0 - 6.5	______
6.5 - 7.5	______
≥ 7.5	______

*Do not include upper energy limit of each group in summation.

Internal Distribution

1-3. L. S. Abbott
4. A. R. Buhl
5-9. C. E. Clifford
10. M. L. Gritzner
11. W. O. Harms
12. R. E. Maerker
13. F. C. Maienschein
14. B. J. McGregor
15. F. R. Mynatt
16. E. M. Oblow
17. F. G. Perey
18. R. W. Roussin
19. A. H. Snell
20. D. B. Trauger
21. D. K. Trubey
22. G. E. Whitesides
23-72. Radiation Shielding Info. Ctr.
73. H. Feshbach (consultant)
74. P. F. Fox (consultant)
75. H. Goldstein (consultant)
76. C. R. Mehl (consultant)
77. H. T. Motz (consultant)
78-79. Central Research Library
80. ORNL Y-12 Technical Library Document Reference Section
81-83. Laboratory Records Dept.
84. Laboratory Records ORNL RC
85. ORNL Patent Office

External Distribution

86. H. Alter, Atomics International, 8900 Desota St., Box 309, Canoga Park, California 91304
87. Martin Becker, Rensselaer Polytechnic Institute, Tibbits Ave., Troy, N. Y. 12181
88. R. Dannels, Westinghouse Electric Corp., ARD, Waltz Mill Site, P. O. Box 158, Madison, Pa. 15663
89. M. Drake, Brookhaven National Laboratory, Upton, N. Y. 11973
90. N. Francis, Knolls Atomic Power Laboratory, Schenectady, N. Y. 12301
91. R. A. Grimesey, Idaho Nuclear Corp., P. O. Box 1845, Idaho Falls, Idaho 83401
92. W. H. Hannum, Division of Reactor Development & Technology, U. S. Atomic Energy Commission, Washington, D. C. 20545
93. P. B. Hemmig, Division of Reactor Development & Technology, U. S. Atomic Energy Commission, Washington, D. C. 20545
94. L. Harris, Gulf General Atomic, P. O. Box 608, San Diego, California 92112
95. B. Hutchins, General Electric Co., BRDO, 310 DeGuigne Drive, Sunnyvale, California 94086
96. M. H. Kalos, Courant Institute of Mathematical Sciences, New York University, 251 Mercer Street, New York, N. Y. 10012
97. D. C. Kaul, Defense Nuclear Agency, Washington, D. C. 20305
98. R. J. LaBauve, Los Alamos Scientific Laboratory, P. O. Box 1663, Los Alamos, New Mexico 87544
99. K. O. Laughon, AEC Site Representative, ORNL
100. Duane Marr, WADCO, P. O. Box 1970, Richland, Washington 99352
101. Malcolm McGregor, Lawrence Livermore Laboratory, Berkeley, California 94720

102. T. A. Pitterle, Westinghouse Electric Corp., ARD, Waltz Mill Site, P. O. Box 158, Madison, Pennsynvania 15663
103. D. L. Rigotti, U. S. Army Nuclear Defense Laboratory, P. O. Box 856, Edgewood Arsenal, Maryland
104. E. Specht, Atomics International, 8900 Desota Street, Box 309, Canoga Park, California 91304
105. E. A. Straker, Science Applications, Inc., Clinton Bldg., Suite 700, 2109 West Clinton Avenue, Huntsville, Alabama 35805
106. A. Travelli, Argonne National Laboratory, 9700 South Cass Avenue, Argonne, Illinois
107-116. Sol Pearlstein, NNCSC, Brookhaven National Laboratory, Upton, New York 11973
117-118. Technical Information Center (TIC)
119. Research and Technical Support Division